

# In-situ elevated-temperature TEM study of $(\text{AgSbTe}_2)_{15}(\text{GeTe})_{85}$

Bruce A. Cook · Xuezheng Wei · Joel L. Haringa ·  
Matthew J. Kramer

Received: 2 August 2006 / Accepted: 2 April 2007 / Published online: 20 June 2007  
© Springer Science+Business Media, LLC 2007

**Abstract**  $(\text{AgSbTe}_2)_{15}(\text{GeTe})_{85}$  (TAGS-85) is a p-type semiconductor characterized by a maximum dimensionless thermoelectric figure of merit of 1.4–1.7 at elevated temperature. In this study, the microstructure of as-solidified TAGS-85 at room temperature and elevated temperature (160 °C) was investigated using TEM. At room temperature, pervasive twinning was observed throughout the specimen. Upon heating to above 120 °C, some of the twins dissolved and new point defects began to nucleate. The mechanisms responsible for formation of high temperature defects are discussed.

## Introduction

Germanium-telluride based semiconductors of the form  $(\text{AgSbTe}_2)_{1-x}(\text{GeTe})_x$  have been of interest for thermoelectric energy conversion since the early 1960s. Dismukes, Rosi, and Hockings reported a large density of states effective mass in the  $(\text{AgSbTe}_2)$  ternary alloy system, which gives rise to a large Seebeck coefficient. Subsequent efforts to reduce the lattice thermal conductivity through solid solution alloying identified two promising compositions,  $(\text{AgSbTe}_2)$ – $(\text{GeTe})$  and  $(\text{AgSbTe}_2)$ – $(\text{PbTe})$ . In fact, early research identified one of the heretofore lowest lattice

thermal conductivity values at 300 K, 4.5 mW/cm K, in solid-solution alloys of compound semiconductors within the  $(\text{AgSbTe}_2)$ – $(\text{PbTe})$  system [1]. Microstructural studies of nominally single-phase  $\text{AgSbTe}_2$  revealed the presence of platelike epitaxial  $\text{Sb}_2\text{Te}_3$  precipitates, parallel to the {111} planes of the  $\text{AgSbTe}_2$  matrix [2], indicating incongruent melting. However, not all researchers reported the existence of such features. The discovery of a high dimensionless thermoelectric figure of merit (ZT) of ~1 at 650 K associated with the 90 mol%  $(\text{GeTe})$  composition motivated subsequent studies on the  $(\text{GeTe})$ -rich compositions [1]. While researching various  $(\text{GeTe})$ : $(\text{AgSbTe}_2)$  ratios, Skrabek et al. observed an unexpected discontinuous decrease in the thermal conductivity at the 80 and 85 mol%  $(\text{GeTe})$  compositions, which occurred without a concomitant decrease in electrical conductivity or Seebeck coefficient. As a result, the ZT at 750 K corresponding to these compositions was reported to reach a value of 1.4 and 1.5 for the 85 and 80%  $(\text{GeTe})$  compositions, respectively [3].

Alloys of the form  $(\text{GeTe})$ : $(\text{AgSbTe}_2)$ , commonly referred to by the acronym “TAGS-m,” where m represents mole percent  $(\text{GeTe})$ , are intrinsically p-type and are typically combined with a  $(\text{PbTe})$  n-leg in a thermoelectric device. As the composition is varied from  $\text{AgSbTe}_2$  to  $(\text{GeTe})$ , the transport properties vary smoothly, except for an anomalous double minimum in thermal conductivity at 80 and 85%  $(\text{GeTe})$ . These minima result in an extremely low lattice thermal conductivity,  $k_l$ , of 0.003–0.010 W/cm K which, when combined with a large carrier mobility,  $\mu$  of 100–200  $\text{cm}^2/\text{V s}$  [4], yields a particularly attractive  $\mu/k_l$  ratio, one of the classical indicators of high ZT in conventional band-type semiconductors [5]. Other researchers have reported ZT values as high as 1.7 in the TAGS-80 composition [6], however, its inferior mechanical strength led to

B. A. Cook (✉) · X. Wei · J. L. Haringa ·  
M. J. Kramer  
Ames Laboratory Materials and Engineering Physics Program,  
Iowa State University, Ames, IA 50011-3020, USA  
e-mail: cook@ameslab.gov

M. J. Kramer  
Department of Materials Science and Engineering, Iowa State  
University, Ames, IA 50011-3020, USA

more widespread use of TAGS-85,  $(\text{AgSbTe}_2)_{15}(\text{GeTe})_{85}$ , as the preferred composition. It has been widely recognized that this material undergoes a polymorphic transformation above 300 K, from a low-temperature rhombohedral ( $R_{3m}$ ) to a high-temperature cubic ( $F_{m-3m}$ ) structure, the transition temperature depending primarily on the ratio of GeTe to  $\text{AgSbTe}_2$  and also on the ratio of Sb to Ag. Abrikosov et al. conducted X-ray diffraction and dilatometric studies on GeTe with controlled additions of  $\text{AgSbTe}_2$  and concluded that the  $\alpha$  (rhombohedral)  $\rightarrow$   $\beta$  (cubic) transition temperature occurs over the temperature range 450–525 K, within the typical operating temperature range of the material in thermoelectric applications [7].

Detailed microstructural studies on GeTe were performed by Snykers et al., who interpreted the material's inherently low fracture toughness in terms of the formation of a domain structure, associated with the  $\alpha$  to  $\beta$  transformation [8]. In the high temperature NaCl polymorph, the Ge and Te atoms occupy the 4a Wyckoff position, with Te at the (0,0,0) and Ge at the  $(\frac{1}{2}, \frac{1}{2}, \frac{1}{2})$  positions. In the TAGS composition, Ag and Sb substitute for Ge, on the  $(\frac{1}{2}, \frac{1}{2}, \frac{1}{2})$  positions. As the material is cooled through the transformation temperature, thermal strain in the NaCl-type lattice is accommodated by a slight shift in the position of the Ge and Te atoms within the (220) planes. The shift manifests itself as a distortion along the [111] direction in the unit cell, producing the rhombohedral  $R_{3m}$  structure. As a consequence, the (220) Bragg peak becomes split into a doublet. The rhombohedral angle in this structure is  $88^\circ$ , a  $2^\circ$  distortion from the  $90^\circ$  cubic polymorph [9]. As a consequence of the degeneracy due to the rhombohedral distortion, the {110} mirror planes within the cubic system are now potential twin planes. The twins, associated exclusively with the low-temperature  $R_{3m}$  polymorph, are not consistent with the high-temperature  $F_{m-3m}$  structure.

Recently, Kanatzidis et al. have reported ZT values near 1.7 at 700 K in related systems,  $(\text{AgSbTe}_2)_{9.09}(\text{PbTe})_{90.91}$  and  $(\text{AgSbTe}_2)_{5.26}(\text{PbTe})_{94.74}$  [10]. These results represent the highest ZT reported to-date in bulk thermoelectric materials. It has been proposed that one mechanism responsible for the low lattice thermal conductivity in these alloys is the presence of nanoscale compositional modulations, either in the form of inclusions (i.e., quantum dots) or in the form of sheets or lamellae. Given the chemical similarity between the two classes of materials, it is anticipated that a detailed study of the TAGS structure may provide insights into microstructural phenomena common to both systems. Therefore, the objective of this study was to investigate the structure of TAGS-85 alloys using transmission electron microscopy and high temperature X-ray diffraction, and to characterize the high-temperature stability of microstructural defects using an in-situ hot stage.

## Experimental

Specimens of TAGS-85 were prepared by direct reaction of the constituent elements in sealed quartz ampoules. Stoichiometric quantities of Te (Cabot, 6N), Ge, (Atlantic Equipment Eng., 5N), Ag (Engelhard, 4N), and Sb (Cerac, 5N), were weighed out in a glove box to a nominal mass of 40 g. The ampoules were sealed under argon and heated to 1,098 K for 1 h, cooled to 773 K and held for 48 h before furnace-cooling to 300 K. While at 1,098 K, the ampoules were periodically withdrawn from the furnace and rocked to thoroughly mix the liquid. After cooling, the ampoules were inspected and no evidence of reaction with the sample was observed. The product was a silvery ingot, possessing millimeter-sized grains clearly visible to the eye. High-temperature X-ray diffraction patterns were obtained at MUCAT beamline 6-ID-D at the Advanced Photon Source, Argonne National Laboratory. The sample was ground and sieved to  $-325$  mesh and sealed in a 2 mm quartz capillary tube. The tube was heated at a constant heating rate of  $10^\circ\text{C}/\text{min}$  from room temperature to 873 K ( $600^\circ\text{C}$ ), while being rotated continuously at  $\sim 20$  rpm. The diffraction condition was transmission, using high-energy synchrotron radiation,  $\sim 100$  keV ( $\lambda = 0.12347 \text{ \AA}$ ). Data was collected using a MAR-165 CCD in an offset position so as to collect a  $60^\circ$  degree arc of the Debye rings. Exposure was 25 s with exposures sequentially taken  $\sim 1$  every  $5^\circ\text{C}$ . Specimens for TEM examination were obtained by sectioning slices from the ingot with a low speed diamond saw, followed by mechanical grinding to  $\sim 200 \mu\text{m}$ , dimpling to less than  $40 \mu\text{m}$ , and then ion milling to perforation using a Gatan model 600 ion mill. The specimens were examined in a Philips CM-30 TEM operated at 300 kV. Following examination at room temperature, the foils were heated to  $160^\circ\text{C}$  using an in-situ Gatan model 628 double tilt hot stage.

## Results and discussion

The room temperature and  $327^\circ\text{C}$  X-ray diffraction patterns for as-solidified TAGS-85 are shown in Figs. 1a and b, respectively. All peaks were indexed to either the low-temperature rhombohedral or high-temperature cubic polymorph. The characteristic splitting of the (220) Bragg reflection of the  $R_{3m}$  phase, discussed below, can be seen in the room temperature pattern.

The value of the rhombohedral angle,  $\alpha$ , was calculated according to Eq. (1):

$$\alpha = 2 * \sin^{-1} (3 / ((2 * (3 + (c^2/a^2)))^{0.5})) \quad (1)$$

From this calculation, it was determined that the transformation during heating was complete at 510 K ( $237^\circ\text{C}$ ).

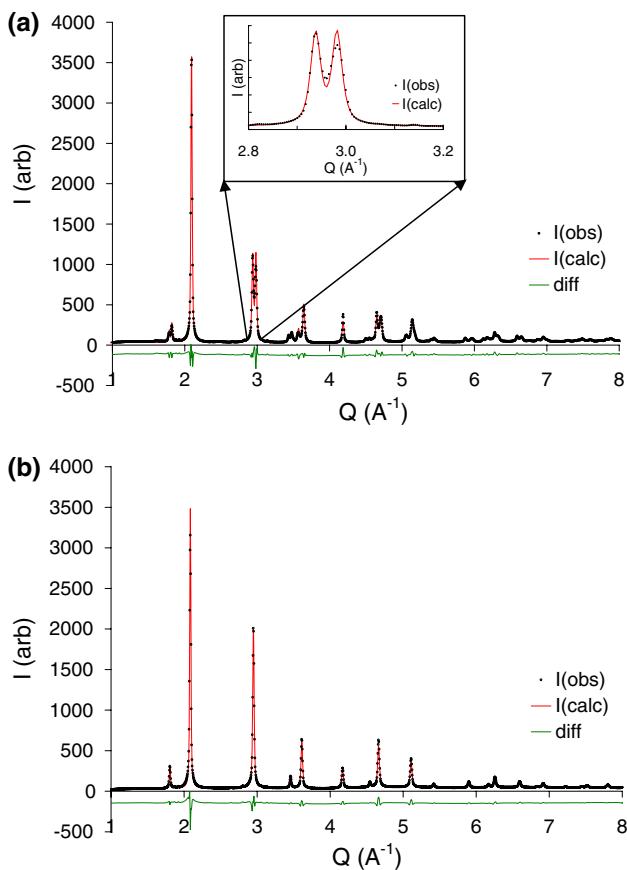


**Fig. 1** X-ray diffraction patterns and their Rietveld refinement of as-solidified TAGS-85; (a) 47 °C (320 K), (b) 327 °C (600 K). Note the presence of the {220} doublet associated with the low-temperature polymorph (shown in the inset of (a)). (The reciprocal distance is in  $Q$  (wave momentum number where  $Q = 4\pi\sin(\theta)/\lambda$ )

The as-solidified microstructure of TAGS-85 is characterized by extensive twinning along the {220} planes, as shown in the TEM bright field micrograph of Fig. 2a. An area of the sample containing twins in two complementary orientations ( $\sim 90^\circ$ ) was selected and the tilts were adjusted to provide a good two-beam image which showed the twins in contrast. The corresponding selected area electron diffraction pattern along the [001] zone axis is shown in Fig. 2b.

A range of twin spacing was observed; the micrograph shown in Fig. 2 is representative of a region of larger spacing. These twins have a maximum characteristic spacing ranging from 450–500 nm and are pervasive throughout the material, as expected as a consequence of the inherent formation mechanism associated with the crystallographic distortion. Most twins were found to terminate on grain boundaries or form as clusters of interpenetrating polysynthetic twins. While the twins are purely structural modulations, numerous antiphase domains are also observed throughout the material, which correspond to compositional fluctuations. Antiphase domains appear to

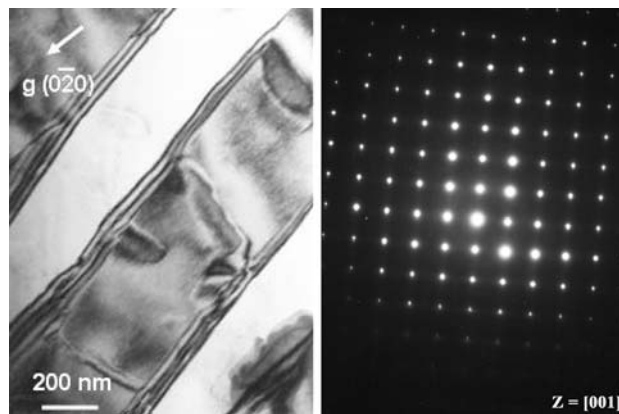


**Fig. 2** (a) Bright field image of twin structures associated with the rhombohedral polymorph of TAGS-85. (b) SAED of the rhombohedral polymorph of TAGS-85 on [001] zone

form immediately upon solidification; when the cells transform from high temperature cubic to the low temperature rhombohedral polymorph, the twins that form appear to cut through pre-existing antiphase domains. The antiphase domains are typically elongated with dimensions of  $\sim 250 \times \sim 100$  nm with an average separation of  $\sim 1$   $\mu\text{m}$ .

As the sample was heated using an in-situ hot stage, the microstructure changed appreciably as the phase contrast of the twins disappeared. There were also obvious changes to the foil edge, where initially smooth boundaries quickly became faceted. At 436 K (163 °C) it was impossible to discern any of the twins where the electron beam had been maintained during heating, even though prior high-temperature X-ray diffraction studies indicated that the cubic phase forms at 237 °C [9]. The bright-field image revealed considerable diffraction contrast associated with small elliptical regions, as shown in Fig. 3.

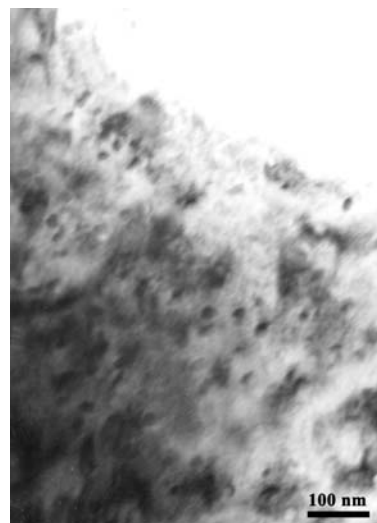


**Fig. 3** Point defects in TAGS-85 TEM foil at 160 °C



**Fig. 4** Bright field image of TAGS-85 at room temperature following in-situ heating to 163 °C. Note the retained point defects after thermal cycling

The foil was repositioned to a new region while maintaining constant temperature and twins were again observed, but these would also fade within a few minutes. At a temperature of 200 °C the vapor pressure of Te is reported as  $2 \times 10^{-7}$  Torr, which is the highest of any of the four constituent elements comprising this compound. The observations from this study suggest that in the thin regions of the foil, where there is a high surface-to-volume ratio, there is a loss of volatile material (Te) under the combined effects of vacuum, ambient heating and a high-energy electron beam. This was further confirmed when observing other areas after cooling back down to room temperature; many of the thin areas lacked obvious twins, however, twins were observed in the thicker regions, as shown in Fig. 4.

A TGA study on a related compound,  $\text{Ag}_{0.85}\text{SnSb}_{1.15}\text{Te}_3$ , revealed no observable loss of material to 700 °C. However, when viewed in the context of this study, the surface-to-volume ratio of ground powder of a typical size employed for TGA studies would be considerably smaller than that of an electron-transparent foil suitable for TEM studies, leading to an increased tendency for loss of high vapor pressure constituents during heating. Moreover, even though most of the electrons pass completely through a TEM foil without dissipating their energy in the material, a fraction are diffracted with a corresponding energy loss. While the actual area of energy dissipation is small, the effect can be quite large because of the high specific energy

deposited ( $\text{J}/\text{nm}^2$ ), which could induce significant changes in the local chemistry. The phase contrast in the thinner regions resulting from heating of the TEM specimen was retained after cooling to room temperature, indicating that the effect is irreversible. This particular type of thermal damage may not manifest itself in the bulk samples, because of the lower surface to volume ratio. Deposition of a thin layer of amorphous carbon on both sides of the foil may ameliorate the difficulty associated with in-situ examination of these materials at elevated temperature.

## Conclusion

Examination of  $(\text{AgSbTe}_2)_{15}(\text{GeTe})_{85}$  (TAGS-85) in a TEM revealed extensive twinning within the  $\{220\}$  crystallographic planes, associated with the room temperature rhombohedral polymorph. The twins possess a characteristic spacing ranging from 450 to 500 nm, and are accompanied by numerous antiphase domains, which are believed to form during solidification from the melt. Attempts to follow the rhombohedral to cubic transformation using an in-situ heating stage revealed preferential loss of volatile material from the high surface to volume ratio foils, leading to irreversible compositional modulations.

**Acknowledgments** The Ames Laboratory is operated for the U. S. Department of Energy by Iowa State University under contract W-7405-ENG-82. This project was supported by the Office of Naval Research, contract no. N00014-05-IP-20065, monitored by Dr. Mihal Gross.

## References

1. Rosi FD, Dismukes JP, Hockings EF (1960) *Electr Eng* 79:450
2. Anderson RW, Faust JW, Tiller WA (1960) *J Appl Phys* 31:1954
3. Skrabek E, Trimmer D (1976) Thermoelectric device including and alloy of GeTe and AgSbTe<sub>2</sub> as the p-type element. U. S. Patent No. 3,945,855, issued March 23, 1976
4. Wood C (1988) *Rep Prog Phys* 51:459
5. Chasmar RP, Stratton R (1959) *J Electron Control* 7:52
6. Christakudis G, Plachkova S, Shelimove L, Avilov E (1991) *Phys Stat Sol* 128:465
7. Kh. Abrikosov N, Dimitrova SK, Karpinskii OG, Plachkova SK, Shelimova LE (1984) *Inorg Mater* 20:42
8. Snykers M, Delavignette P, Amelinckx S (1972) *Mat Res Bull* 7:831–839
9. Cook BA, Kramer MJ, Wei X, Haringa JL, Levin E (2007) *J Appl Phys* 101:053715
10. Hsu KF, Loo S, Guo F, Chen W, Dyck J, Uher C, Hogan T, Polychroniadis E, Kanatzidis M (2004) *Science* 303:818